Algorithm for estimating derating of induction motors supplied with under/over unbalanced voltages using response surface methodology

Merve Sen Kurt[1], *Murat E. Balci*[2], *Shady H.E. Abdel Aleem*[3]

[1]*Electrical and Electronics Engineering Department, Amasya University, Amasya, Turkey*
[2]*Electrical and Electronics Engineering Department, Balikesir University, Balikesir, Turkey*
[3]*Mathematical, Physical & Engineering Sciences Department, 15th of May Higher Institute of Engineering, 15th of May City, Cairo 11731, Egypt*
E-mail: shossam@theiet.org

Published in *The Journal of Engineering*; Received on 21st January 2017; Accepted on 18th July 2017

Abstract: One of the adverse effects of unbalanced three-phase voltages on the induction motors (IMs) is overheating of the windings. The IMs should be loaded at less than their rated power in case of unbalanced supply voltages to prevent this overheating. Recent studies have pointed out that the maximum allowable loading ratio or derating factor (DF) of the IMs have various values for several combinations of the magnitude and angle of the complex voltage unbalance factor (CVUF) operating with a combination of unbalanced over- and under-voltage cases. This means that determination of DF requires plenty of experimental efforts for all possible unbalanced voltage conditions. In this study, the effective root-mean-square voltage definition which is defined in IEEE Standard 1459 is combined with the CVUF for proper identification of over and under unbalanced voltage conditions. An algorithm based on response surface methodology is proposed to estimate a precise DF for a broad range of unbalanced supply voltages. The simulation results are presented to validate the effectiveness of the proposed algorithm. It is apparently figured out that the proposed algorithm has better accuracy compared with the conventional approach reported in National Equipment Manufacturer's Association Standard MG1.

1 Introduction

Voltage unbalance is a power quality problem that can be explained as 'a condition in a poly-phase system in which the root-mean-square (rms) values of the fundamental components of the line voltages, and/or the phase angles between consecutive line voltages, are not all equal' [1]. It always exists in electrical power networks due to the irregular distribution of single-phase loads over the three phases, single-phase distributed resources, power system faults, asymmetry of lines, unbalanced power system faults and others [2]. In the literature, several studies [3–8] reported that voltage unbalance causes efficiency and power factor reduction, torque pulsations and overheating in the windings of the induction motors (IMs). In particular, overheating problem degrades the performance and hastens ageing process of a three-phase motor.

As per the National Equipment Manufacturer's Association (NEMA) Standard MG-1 [9], the amount of voltage unbalance is quantified by the line voltage unbalance rate (LVUR), which is calculated as the ratio of the maximum line voltage deviation to the average of three line voltages' rms values. Besides, the same standard also recommended that IMs should not operate at LVUR values above 5%. For the unbalanced supply voltages with LVUR values between 1 and 5%, a maximum loading ratio given as a function of LVUR curve is provided to avoid the IM's overheating problem [10, 11]. This loading ratio is commonly known as the derating factor (DF). As well, the IEC Standard 60034-26 [12] introduces an index called as voltage unbalance factor (VUF). It is calculated as the ratio of the negative-sequence voltage component (V_-) to the positive-sequence voltage component (V_+). As per [12], the motor supply voltage's unbalance factor should not exceed 2%.

In addition to the NEMA and IEC standards, IEEE Standard 141 [13] accepts the NEMA definition as a measure of the voltage unbalance, but with a small change as the IEEE Standard 141 considers the phase-to-neutral voltages instead of the line voltages for the implementation of the definition.

Other studies interpreted that the voltage unbalance indices defined by the standards mentioned above are not unique [6, 7, 14]. In other words, the same values of indices can be observed for different unbalanced voltage conditions which cause different overheating in the windings of the IM. As a result, the DF values, which are determined as a function of the indices, may not protect the motor accurately against overheating in some unbalanced voltage cases. Therefore, for precise determination of the DF values of an IM operates under various unbalanced three-phase voltages; a complex VUF (CVUF) was proposed in [15]. The CVUF is an extension of the IEC definition, but it considers both magnitude and angle of the negative-sequence and positive-sequence voltage components. Also, Gnacinski [15] pointed out that the CVUF's angle should be taken into consideration for derating of an IM since it has a significant influence on the winding temperature rise.

Reference [16] noted that the same CVUF value might be observed for both unbalanced under-voltage and over-voltage cases. Accordingly, the same study suggested that the mean value of the line voltages and CVUF should collectively be employed to express the correct voltage unbalance condition. Consequently, a particular DF value could be determined for each voltage unbalance condition.

Similarly, Anwari and Hiendro [17] collectively consider the ratio of positive-sequence voltage to the mean value of the phase voltages, and the CVUF, as a coefficient for describing the voltage unbalance conditions. It was concluded from the parametric analysis presented by Anwari and Hiendro [17] that the VUF, and the coefficient of voltage unbalance can be implemented to evaluate total loss, efficiency, power factor and output torque, precisely. Hence, the CVUF, which consists of both magnitudes (VUF) and angle (θ_V), and the defined voltage unbalance coefficient might be handled together for accurate determination of the derating of an IM.

The most significant result presented in [11, 18] is that the NEMA standard's expression may not be enough to inspect the accurate DF values for all unbalanced supply voltage conditions and IM types. Also, some studies [19, 20] indicated that the machine properties such as slots types and amount of the magnetic circuit's saturation have a significant influence on the DF.

Henceforth, it can be figured out that DF is a function of three parameters: the magnitude (VUF), angle (θ_V) of the CVUF index and the voltage level. Thus, one can see that the determination of DF values under various possible voltage unbalance cases require extensive experimental and computational efforts.

In this paper, the effective rms voltage definition (V_e), which is defined in IEEE standard 1459–2010 [21–23], is combined with the CVUF for proper identification of over unbalanced voltages and under unbalanced voltage conditions. The DF is evaluated for several values of VUF, θ_V of the CVUF and the V_e using simulations based on the *d–q* dynamic model of an IM. Accordingly, the response surface methodology (RSM) [24] is employed as an experimental and computational efficient tool to estimate an expression of the DF in terms of VUF, θ_V and V_e based on the observed relations among the three quantities and the DF. The purpose of the RSM is to use a sequence of experiments to obtain an optimal expression for the DF of the IM. The simulation results are provided to show the validity of the proposed algorithm. The results indicate better accuracy compared with the NEMA standard approach.

The rest of this paper is organised as follows. Section 2 describes the parametric analysis of the derating expression of IMs. The simulated system and its results are explained in details in Section 3. Section 4 describes the proposed method using RSM and its results. Validation of the proposed algorithm is presented in Section 5. Finally, Section 6 is devoted for the conclusions of this work.

2 Parametric analysis of DF of IMs

Fig. 1 shows the DF curve provided by NEMA MG-1 [9]. The DF curve is based on the expression given in (1) [10, 11]

$$1+\frac{2(\mathrm{LVUR}(\%))^2}{100}=\left(\frac{\mathrm{DF}(\%)}{100}\right)^{-1.7} \tag{1}$$

In addition, the expression of the VUF introduced by the IEC Standard 60034-26 [12], and its complex form extension, CVUF, presented in [15], are given as follows:

$$\mathrm{VUF}(\%)=\frac{V_-}{V_+}\times 100 \tag{2}$$

$$\mathrm{CVUF}(\%)=\frac{V_-\angle\theta_{V-}}{V_+\angle\theta_{V+}}\times 100=\mathrm{VUF}(\%)\angle\theta_V \tag{3}$$

In (3), $V_-\angle\theta_{V-}$ and $V_+\angle\theta_{V+}$ denote the phasors of the negative-sequence and positive-sequence voltage components, respectively.

Regarding the voltage level, a mean value of the three-phase rms voltages is frequently employed to describe unbalanced over and under-voltage cases [16, 17]. However, in this paper, the voltage level is measured by considering the effective voltage definition (V_e) [21, 22] given in (4) due to the fact that V_e can be expressed in terms of V_+ and VUF; accordingly, it is much more appropriate for the parametric analysis of the derating expression when compared with the mean value of the three-phase voltages

$$\begin{aligned}V_e&=\sqrt{\frac{V_{ab}^2+V_{bc}^2+V_{ca}^2}{9}}=\sqrt{V_+^2+V_-^2}\\&=V_+\sqrt{1+\left(\frac{\mathrm{VUF}(\%)}{100}\right)^2}\end{aligned} \tag{4}$$

To validate the uniqueness of VUF, CVUF and the considered voltage unbalance indicator (the CVUF index combined with V_e), a preliminary assessment for numerous unbalanced line-to-line voltages, is performed. The results given in Fig. 2*a* show that several combinations of three-phase line voltages can be observed for VUF (%) equals 5. Similarly, the results given in Fig. 2*b* show that fewer combinations of three-phase line voltages can be observed for CVUF (%) equals $5\angle -130^\circ$. On the other hand, Fig. 2*c* shows that there is only one possible combination of three-phase line voltages for CVUF (%) equals $5\angle -130^\circ$ and V_e equals 0.9 pu. This means that the CVUF index combined with V_e can fulfil the gap of VUF and CVUF indices, and it can be used as a tool for precise identification of the voltage unbalance cases.

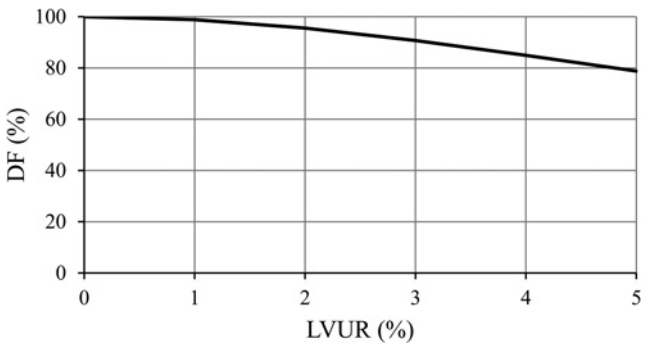

Fig. 1 *DF curve provided by NEMA standard MG-1*

3 Simulated system and results

In this section, under various supply voltage unbalance conditions, derating of the IMs is parametrically investigated with the aid of the simulations. The results of the parametric analysis are important to realise the variation of DF for different voltage unbalance cases with different magnitudes of VUF and θ_V values of the CVUF, and different voltage levels.

The system under study is given in Fig. 3. It consists of three single-phase voltage source, three-phase squirrel cage IM and a set of blocks for the measurements of the rms voltages, rms currents, positive-sequence and negative-sequence voltage components, the instantaneous angular rotor speed [$\omega_r(t)$] and the instantaneous mechanical torque [$T_m(t)$].

The loading ratio of the IM can be calculated in terms of the measured $\omega_r(t)$ and $T_m(t)$, as follows:

$$\text{loading ratio }(\%)=\frac{1/T\int_0^T T_m(t)\omega_r(t)\mathrm{d}t}{P_{\text{rated}}}100 \tag{5}$$

where T is the oscillation period and P_{rated} is the IM's rated power.

The simulated IM has nameplate ratings such as 1.5 kW, 380 V, 50 Hz and 925 rpm. Its nameplate ratings, as well as the results of its no-load and locked rotor tests, are given in the Appendix, Fig. 7. In the simulations, the IM is represented using the popular *d–q* dynamic model that is available in the MATLAB/simulink library. It should be underlined that the *d–q* model has been well tested in the literature, and it has been proven that it is considered reliable for both steady state and transient analysis [18, 25–27].

Basically, the DF can be explained as the IM's maximum allowable loading ratio under unbalanced supply voltage conditions in which no damage is imposed to the IM. In the literature, it is determined when the highest phase current does not exceed the motor's rated current. In this paper, for a precise determination of the DF, the highest stator phase current is intentionally reduced to the rated current by decreasing the motor's loading ratio. Fig. 4 shows the flowchart of the algorithm which is implemented to determine the DF under different unbalanced supply voltage cases.

Two types of parametric analysis are considered to investigate the effect of unbalanced over and under three-phase voltages on the DF of the simulated IM. Type 1 considers constant angle of CVUF, while type 2 considers constant VUF. The details of both

doi: 10.1049/joe.2017.0025

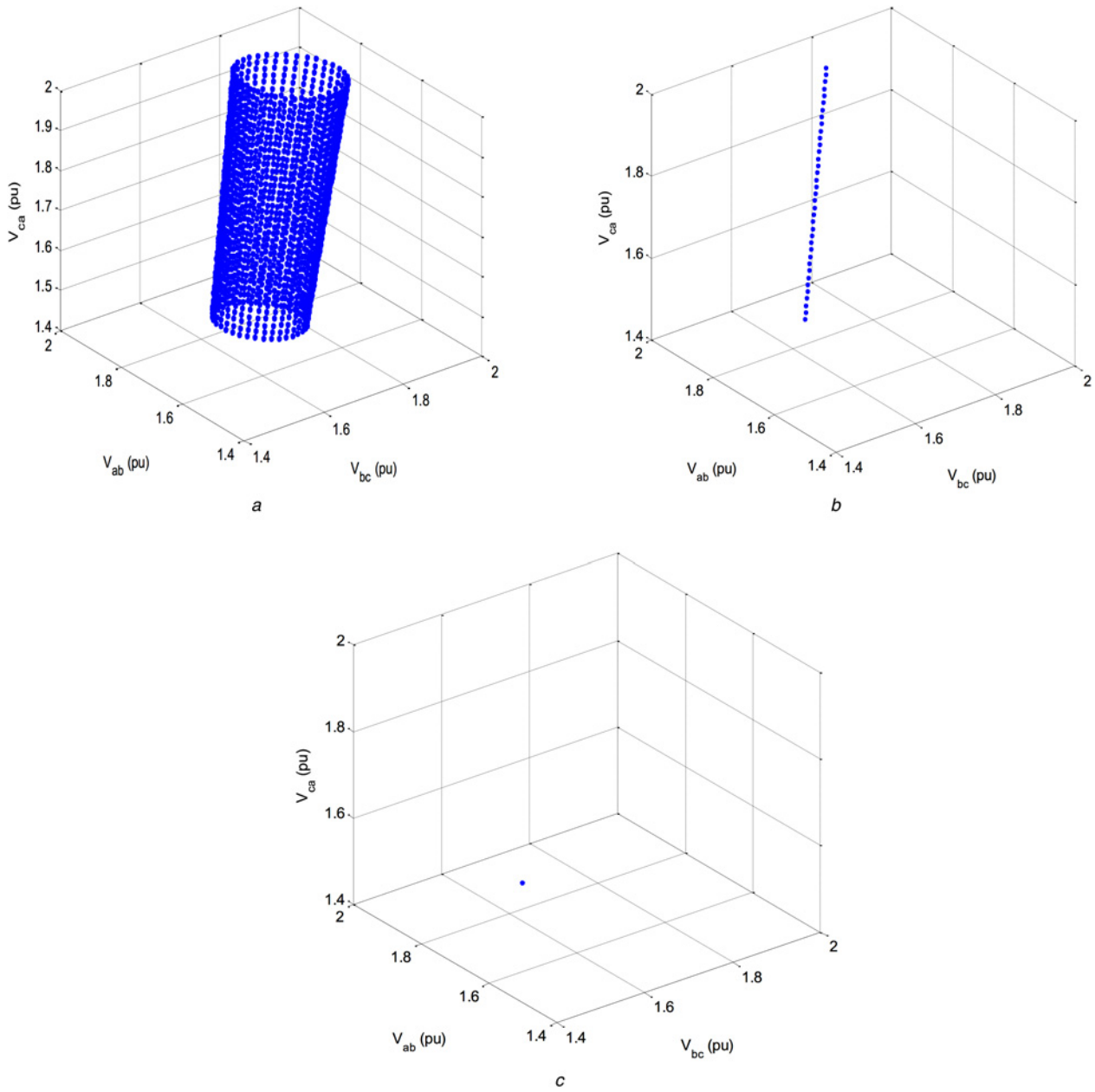

Fig. 2 *Possible combinations of the unbalanced line-to-line voltages*
a VUF (%) = 5
b CVUF (%) = 5∠ − 130°
c CVUF (%) = 5∠ − 130° and V_e = 0.9 pu

types of parametric analysis are given below. Besides, three-phase-to-neutral voltages are generated without the zero-sequence component for both types of analyses due to the fact that this component does not affect the IM's performance:

- *Type 1*: For three voltage levels such as V_e equals 200, 220 and 240 V, VUF (magnitude of CVUF) varies from 0 to 5% when θ_V (angle of CVUF) is kept as 0°.
- *Type 2*: For three voltage levels such as V_e equals 200, 220 and 240 V, θ_V varies from 0° to 360°, while keeping VUF as 5%.

For the test voltages considered in the two types, the DF values are determined by means of the algorithm presented in Fig. 4, and the obtained results are plotted in Figs. 5*a* and *b*. In addition, results of the conventional NEMA standard approach for the three test voltage cases considered in Type 1 with VUF equals 4.5% are presented in Table 1 to be compared with the presented results.

Fig. 5*a* shows that the DF is determined as 100% for the rated balanced voltage condition, i.e. V_e = 220 V and VUF = 0%. For the balanced under-voltage condition (V_e = 200 V and VUF = 0%), the motor should be loaded at less than its rated power with a DF equals 91.33%. In addition, for the balanced over-voltage condition (V_e = 240 V and VUF = 0%), the motor can be loaded at higher than its rated power with a DF = 105.35%. The same figure points out that DF is inversely proportional to the VUF, and the slope of DF–VUF curves increases with V_e. It can be pointed out from Fig. 5*b* that for the same V_e and VUF values, the DF curve is oscillated with θ_V, and the oscillation period of the DF is 120°. This means that the DF has maximum and minimum values of the considered V_e and VUF cases.

Table 1 reveals that the LVUR index and the DF_{NEMA} that is calculated via the NEMA expression given in (1) have the same values (4.54 and 81.60%) for all cases. In addition, for the derating based on the NEMA expression, the observed ratios of the maximum rms

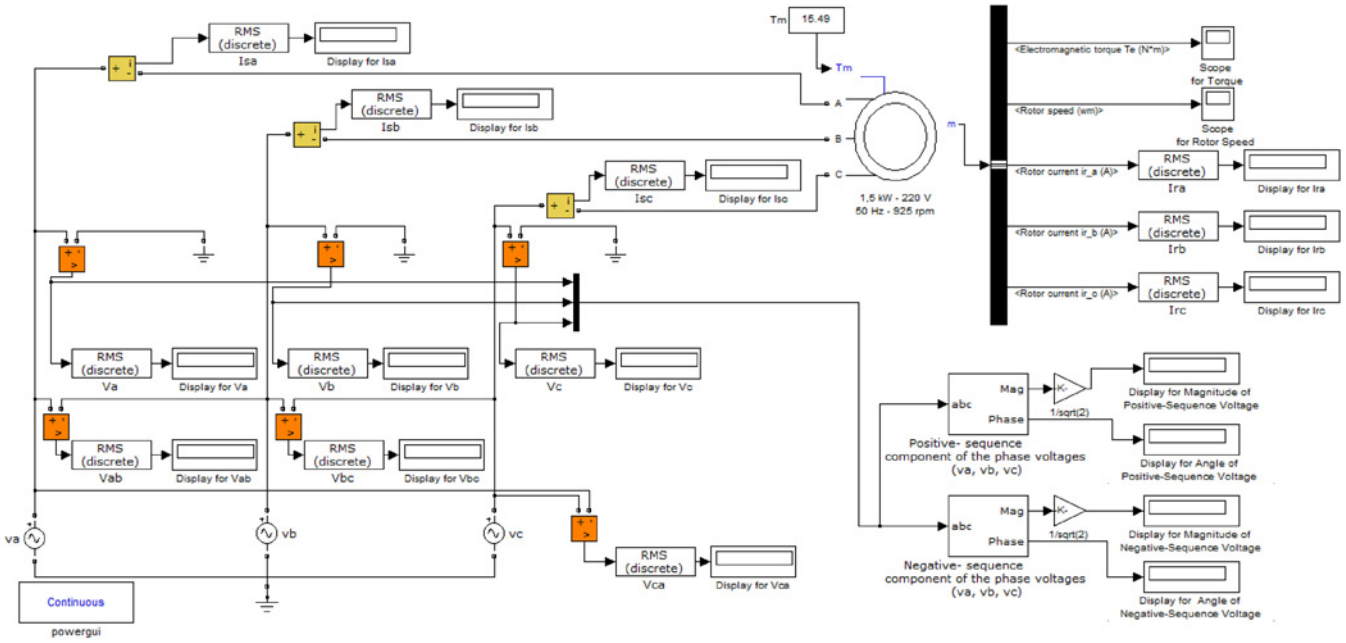

Fig. 3 *Simulated system in the MATLAB/Simulink environment*

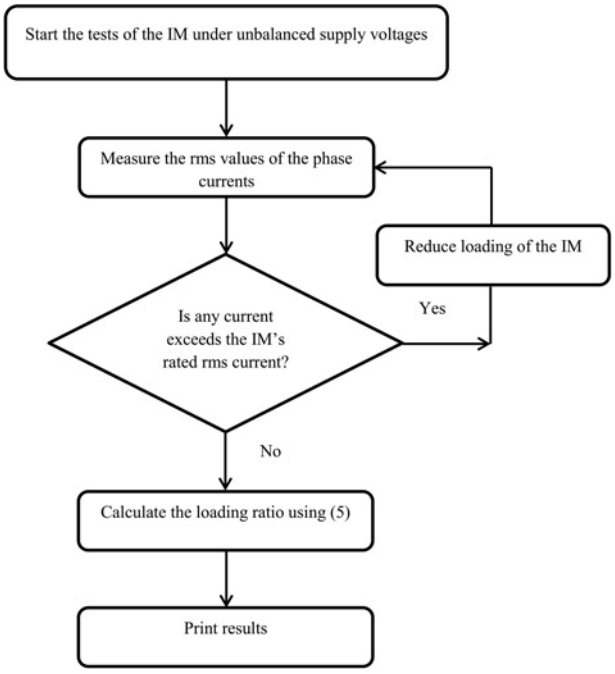

Fig. 4 *Flowchart of the algorithm to determine the DF*

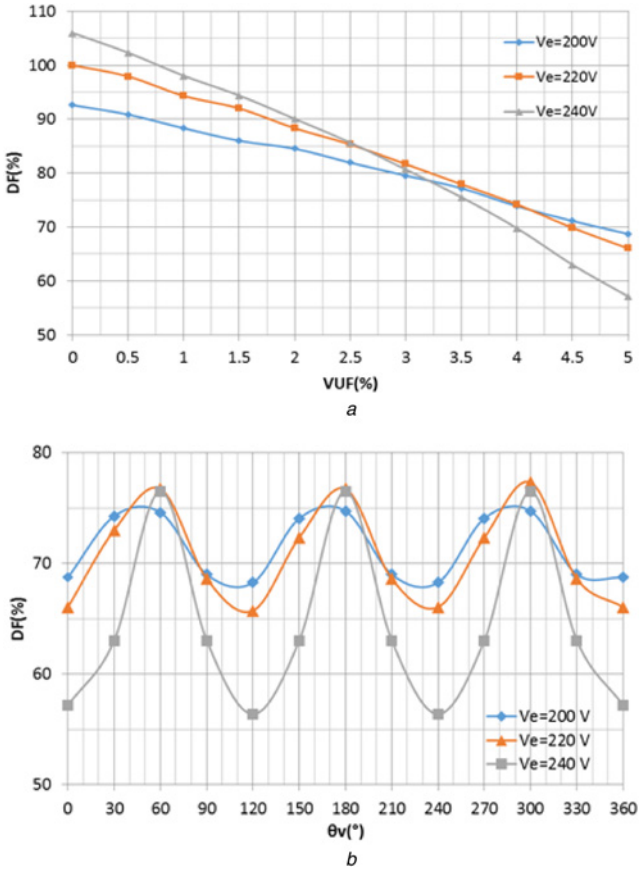

Fig. 5 *DF results obtained from the two types of the parametric analysis*
a Type 1
b Type 2

phase currents to the rated current are 1.06, 1.07 and 1.09 which mean that at least one winding of the IM will be exposed to excessive heat as the current value exceeds the rated current value. As a result, it can clearly be mentioned that the derating based on NEMA standard may not prevent the IM from overheating under the considered unbalanced supply conditions. Accordingly, in this paper, an experimentally and computationally efficient method for the adequate estimation of DF values under a wide range of supply voltage unbalance cases will be proposed by means of the RSM.

4 Proposed method using RSM

RSM is a statistical technique that can be employed to find the mathematical relationships between the outputs (responses) and the inputs of a process with minimum number of experiments [24, 28, 29]. The experimentation is the employment of treatments to experimental units to measure one or more responses for gathering information about how a system (or particular process) works. It plays a major role in engineering, science and domains, especially

doi: 10.1049/joe.2017.0025

Table 1 Results of the conventional NEMA standard approach for the three test voltage cases considered in Type 1 with VUF equals 4.5%

V_e, V	VUF, %	θ_V, °	LVUR, %	DF_{NEMA}, %	$I_{maximum}/I_{rated}$, %
200	4.50	0	4.54	81.60	1.06
220	4.50	0	4.54	81.60	1.07
240	4.50	0	4.54	81.60	1.09

when treatments are from a continuous range of values. In this regard, one of the commonly known methods to find the relationship (response function) between inputs (independent variables) and output (dependent variable) is the RSM.

RSM has three standard types to get the unknown response function, and they are commonly known as the first-order, second-order and three-level fractional factorial models. The first-order model is suitable if the response can be defined by a linear function of independent variables; therefore, it is simple and straightforward, but it is not suitable for most of the real practised problems because of the significant lack of fit. The second-order model is a highly structured and flexible model that can interpret the response surface with a parabolic curvature and finds a good estimation of the true response surface. The three-level fractional factorial model is also a high structured model that can be employed when the parabolic curvature is the primary interest, but the complexity and the excessive number of runs are its main drawbacks when the number of factors (inputs) is significant. Finally, the advantages of the RSM are the understanding of the response surface topography and finding the region where the optimal response occurs [30].

In this work, a second-order multi-regression model is used to estimate the DF values (output of the RSM) under various voltages unbalance cases with the three factors VUF, θ_V and V_e since it was observed from the analysis results presented in the previous section that the DF is a function of these factors. The second-order model is usually expressed as follows:

$$Y_u = \beta_0 + \sum_{i=1}^{n} \beta_i X_{iu} + \sum_{i=1}^{n} \beta_{ii} X_{iu}^2 + \sum_{i<j}^{n} \beta_{ij} X_{iu} X_{ju} + e_u \quad (6)$$

where Y_u is the corresponding response of the uth observation, X_{iu} are coded values of the ith input parameters, i and j are the linear and quadratic coefficients and e_u is the residual experimental error of the uth observation (random error). The terms β_0, β_i, β_{ii} and β_{ij} are the regression coefficients, and they are represented by the coefficient matrix $\boldsymbol{\beta}$, as follows:

$$\boldsymbol{\beta} = (\boldsymbol{X}^{\mathrm{T}}\boldsymbol{X})^{-1}\boldsymbol{X}^{\mathrm{T}}\boldsymbol{Y} \quad (7)$$

where $\boldsymbol{X}$ is a matrix which consists of different combinations of input values for each factor (X_{iu} and X_{ju}) and $\boldsymbol{Y}$ is a matrix which consists of Y_u values.

Numerical results which are obtained by means of the simulation system given in Fig. 3 are employed to estimate and validate the DF expression using the RSM. The implementation of RSM-based DF estimation algorithm is detailed as follows:

(i) Choose initial lower and upper values of the input factors (VUF, θ_V and V_e) as given in Table 2.
(ii) Develop the experiment matrix or experimental region by considering the lower and upper values of the input factors as given in Table 3.
(iii) Find the DF using the algorithm previously described with the flowchart given in Fig. 4 for each supply voltage condition used in the experiment matrix.
(iv) Approximate a function of the response (DF) in terms of the input factors (VUF, θ_V and V_e) using the second-order regression model given in (6) and (7).

Table 2 Factor levels of the inputs (VUF, θ_V and V_e)

Inputs/values	Low value (coded as '−1')	Medium value (coded as '0')	High value (coded as '1')
VUF, %	0	2.5	5
θ_V, °	0	60	120
V_e, V	200	220	240

It is seen from Table 2 that lower and upper values of VUF are 0 and 5%, and upper and lower values of V_e are about ±10% of the IM's rated phase-to-neutral voltage (220 V). On the other hand, due to the fact that the DF curves which are given in Fig. 5*b* have the same replica for each three intervals such as 0–120°, 120–240° and 240–360°; accordingly, the lower and upper values of θ_V are selected as 0° and 120°, respectively.

Considering the results of the 15 experiments given in Table 3, the RSM is performed to establish a DF expression in terms of

Table 3 Developed experiment matrix and the calculated DF values

Inputs	V_e, V		VUF, %		θ_V, °		DF, %
Number	Actual value, V	Coded value	Actual value, %	Coded value	Actual value, deg	Coded value	
1	200	−1	0.0	−1	0	−1	91.33
2	240	1	0.0	−1	0	−1	105.35
3	200	−1	5.0	1	0	−1	69.40
4	240	1	5.0	1	0	−1	58.63
5	200	−1	0.0	−1	120	1	91.33
6	240	1	0.0	−1	120	1	105.35
7	200	−1	5.0	1	120	1	69.40
8	240	1	5.0	1	120	1	58.63
9	200	−1	2.5	0	60	0	85.32
10	240	1	2.5	0	60	0	89.60
11	220	0	0.0	−1	60	0	100.00
12	220	0	5.0	1	60	0	75.30
13	220	0	2.5	0	0	−1	84.77
14	220	0	2.5	0	120	1	84.52
15	220	0	2.5	0	60	0	89.69

the factors with R^2 value of 98.72%, as follows:

$$\begin{aligned}\mathrm{DF}(V_\mathrm{e},\ \mathrm{VUF},\ \theta_\mathrm{V}) = {} & 89.404 + 1.078(V_\mathrm{e}) - 16.200(\mathrm{VUF}) \\ & - 0.025(\theta_\mathrm{V}) - 1.873(V_\mathrm{e})^2 - 1.683(\mathrm{VUF})^2 \\ & - 4.688(\theta_\mathrm{V})^2 - 6.197(V_\mathrm{e})(\mathrm{VUF})\end{aligned} \tag{8}$$

The expression given in (8) is suitable for θ_V values ranges between 0° and 120°; however, for the θ_V interval between 120° and 360°, the updated $\hat{\theta}_\mathrm{V}$ values given in (9) should be used instead of θ_V given in (8)

$$\hat{\theta}_\mathrm{V} = \left\{ \begin{array}{l} \theta_\mathrm{V} - 120^\circ \mathrm{for} 120^\circ < \theta_\mathrm{V} \le 240^\circ \\ \theta_\mathrm{V} - 240^\circ \mathrm{for} 240^\circ < \theta_\mathrm{V} \le 360^\circ \end{array} \right\} \tag{9}$$

For the considered V_e, VUF and θ_V intervals, three-dimensional (3D) DF surfaces are plotted using (8) and (9) as shown in Fig. 6. It can be pointed out from this figure that the surfaces are consistent with the trends of the DF–VUF and DF–θ_V curves which are presented in Figs. 5*a* and *b*.

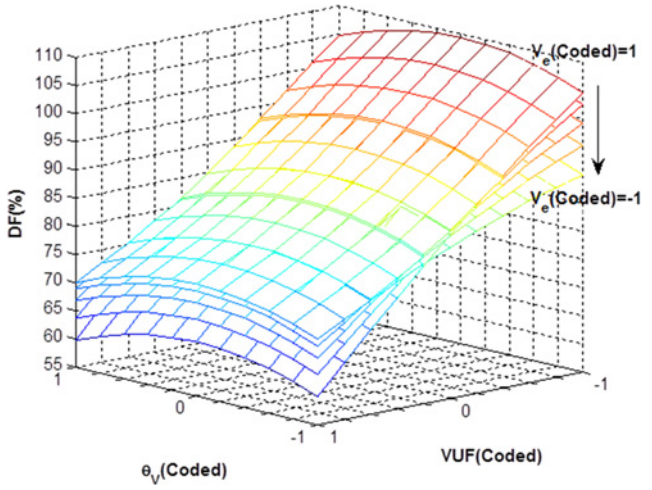

Fig. 6 *3D DF surfaces observed for the considered V_e, VUF and θ_V intervals*

5 Proposed algorithm validation

The DF values predicted using the proposed algorithm and the NEMA's DF expression are compared with the measured DF values for five random unbalanced test voltage cases to confirm the validity of the results obtained with the proposed algorithm. The phase-to-neutral voltages which are generated for the randomly selected test cases are given in Table 4, and the results of the comparative analysis are presented in Table 5.

Table 5 reveals that the proposed algorithm allows adequate prediction of the DF within a wide range of V_e, VUF and θ_V terms. For the tested cases, the maximum difference between the DF values predicted by the proposed algorithm and the directly measured DF values is nearly 3.5%. For the same test cases, the maximum difference between the DF values calculated based on NEMA standard approach and the directly measured DF values is nearly 21.5%. As a result, it can be figured out that the proposed algorithm has a better approximation to the DF values directly determined with the simulations.

6 Conclusion

In this paper, the effective rms voltage definition (V_e) reported in IEEE Standard 1459–2010 is combined with the CVUF for a proper determination of unbalanced voltage conditions. With the aid of the simulations, the DF is evaluated for several values of magnitude (VUF), angle (θ_V) of CVUF and V_e. The numerical results indicate that the DF is inversely proportional to the VUF, and the slope of DF–VUF curve increases with V_e. It is also observed from the results that for constant V_e and VUF values, the DF oscillates with the variation of θ_V and the oscillation period of the DF curve is found to be 120°.

RSM-based algorithm is developed computationally efficient tool to estimate the DF expression regarding V_e, VUF and θ_V of unbalanced voltages, taking into consideration the observed relations between the three quantities and the DF.

The numerical results based on the simulations are also presented to validate the proposed algorithm under a wide range of supply voltage unbalance cases. Finally, it is clearly figured out that for DF estimation, the proposed algorithm has better accuracy compared with the NEMA-MG1 standard approach.

Table 4 Phase-to-neutral voltages employed for the unbalanced test voltage cases

Cases	V_a, V	V_b, V	V_c, V	θ_{Va}, deg	θ_{Vb}, deg	θ_{Vc}, deg
1	237.91	250.99	230.64	2.84	−120.93	118.08
2	206.02	204.48	204.48	0	−120.24	120.24
3	210.81	221.25	212.78	1.34	−119.71	118.36
4	224.70	215.18	220.00	−0.70	−120.73	121.43
5	225.36	239.00	225.36	2.02	−120.00	117.97

Table 5 Comparative analyses for the different DF expressions

Cases	V_e, V	VUF, %	θ_V, °	LVUR, %	DF values, %		
					Measured from simulation	Estimated using the proposed algorithm	Calculated using NEMA approach
1	240	5	100	4.743	59.06	62.42	80.37
2	205	0.5	0	0.493	92.40	91.04	99.71
3	215	3	130	2.982	80.60	82.78	90.82
4	220	2.5	330	2.170	85.33	88.22	94.84
5	230	4	120	4.043	72.06	72.57	84.67

7 Acknowledgment

The authors gratefully acknowledge Mr. Selcuk Sakar for his support during preparation of this paper.

8 References

[1] Mantilla L.F.: 'An analytical and graphical study of the symmetrical components in an induction motor supply in relation to the voltage unbalance parameters', *Electr. Eng.*, 2007, **89**, (7), pp. 535–545
[2] Fuchs E.F., Masoum M.A.S.: 'Power quality in power systems and electrical machines' (Elsevier Academic Press, Burlington, MA, 2008, 1st edn.)
[3] Gnaciński P., Pepliński M.: 'Lowered voltage quality and load-carrying capacity of induction motors', *IET Electr. Power Appl.*, 2016, **10**, (9), pp. 843–848
[4] Ferreira F.J.T.E., Baoming G., de Almeida A.T.: 'Reliability and operation of high-efficiency induction motors', *IEEE Trans. Ind. Appl.*, 2016, **52**, (6), pp. 4628–4637
[5] Duran M.J., Barrero F.: 'Recent advances in the design, modeling, and control of multiphase machines – part II', *IEEE Trans. Ind. Electron.*, 2016, **63**, (1), pp. 459–468
[6] Lee C.Y.: 'Effects of unbalanced voltage on the operation performance of a three phase induction motor', *IEEE Trans. Energy Convers.*, 1999, **14**, (2), pp. 202–208
[7] Youb L.: 'Effects of unbalanced voltage on the steady state of the induction motors', *Int. J. Electr. Energy*, 2014, **2**, (1), pp. 34–38
[8] Faiz J., Ebrahimpour H., Pillay P.: 'Influence of unbalanced voltage supply on efficiency of three phase squirrel cage induction motor and economic analysis', *Energy Convers. Manage.*, 2006, **47**, (3), pp. 289–302
[9] NEMA Standard MG1: 'Motor and generators, part 14.36: effects of unbalanced voltages on the performance of polyphase induction motors', 2009
[10] Pillay P., Hoftmann P., Manyage M.: 'Derating of induction motors operating with a combination of unbalanced voltages and over or under voltages', *IEEE Trans. Energy Convers.*, 2002, **17**, (4), pp. 485–491
[11] Reineri C.A., Gomez J.C., Balaguer E.B., *ET AL.*: 'Experimental study of induction motor performance with unbalanced supply', *Electric Power Comp. and Syst.*, 2006, **34**, (7), pp. 817–829
[12] IEC Standard 60034-26: 'Rotating electrical machines – part 26: effects of unbalanced voltages on the performance of three-phase induction motors', 2002
[13] IEEE Standard 112: 'IEEE standard test procedure for poly-phase induction motors and generators', 1991
[14] Wang Y.J.: 'Analysis of effects of three-phase voltage unbalance on induction motors with emphasis on the angle of the complex voltage unbalance factor', *IEEE Trans. Energy Convers.*, 2001, **16**, (3), pp. 270–275
[15] Gnacinski P.: 'Effect of unbalanced voltage on windings temperature, operational life and load carrying capacity of induction machine', *Energy Convers. Manage.*, 2008, **49**, (4), pp. 761–770
[16] Faiz J., Ebrahimpour H.: 'Precise derating of three phase induction motors with unbalanced voltages', *Energy Convers. Manage.*, 2007, **48**, (9), pp. 2579–2586
[17] Anwari M., Hiendro A.: 'New unbalance factor for estimating performance of a three-phase induction motor with under- and over-voltage unbalance', *IEEE Trans. Energy Convers.*, 2010, **25**, (3), pp. 619–625
[18] Jalilian A., Roshanfekr R.: 'Analysis of three-phase induction motor performance under different voltage unbalance conditions using simulation and experimental results', *Electr. Power Compon. Syst.*, 2009, **37**, (3), pp. 300–319
[19] Gnacinski P.: 'Derating of an induction machine under voltage unbalance combined with over or under voltages', *Energy Convers. Manage.*, 2009, **50**, (4), pp. 1101–1107
[20] Donolo P., Bossio G., De Angelo C.: 'Analysis of voltage unbalance effects on induction motors with open and closed slots', *Energy Convers. Manage.*, 2011, **52**, (5), pp. 2024–2030
[21] IEEE Std. 1459: 'IEEE standard definitions for the measurement of electric power quantities under nonsinusoidal, balanced, or unbalanced conditions', 2010
[22] Balci M.E., Emanuel A.E.: 'Apparent power definitions: a comparison study', *Int. Rev. Electr. Eng.*, 2011, **6**, (6), pp. 2713–2722
[23] Abdel Aleem S.H.E., Ibrahim A.M., Zobaa A.F.: 'Harmonic assessment-based adjusted current total harmonic distortion', *IET J. Eng.*, 2016, pp. 1–9, doi: 10.1049/joe.2016.0002
[24] Montgomery D.C.: 'Design and analysis of experiments' (John Wiley & Sons, Hoboken, NJ, 2009, 7th edn.)
[25] Ozpineci B., Tolbert L.M.: 'Simulink implementation of induction machine model – a modular approach'. Proc. Electronics Machines Drives Conf. (IEMDC 2003), Madison, Wisconsin, USA, June 2003, pp. 728–734
[26] Ayasun S., Nwankpa C.O.: 'Induction motor tests using MATLAB/Simulink and their integration into undergraduate electric machinery courses', *IEEE Trans. Educ.*, 2005, **48**, (1), pp. 165–169
[27] Lee R.J., Pillay P., Harley R.G.: 'D, Q reference frame for the simulation of induction motors', *Electr. Power Syst. Res.*, 1984, **8**, pp. 15–16
[28] Sakar S., Karaoglan A.D., Balci M.E., *ET AL.*: 'Optimal design of single-tuned passive filters using response surface methodology'. Int. School on Nonsinusoidal Currents and Compensation (ISNCC) ISNCC'2015, Poland, June 2015, pp. 1–6
[29] Balci M.E., Karaoglan A.D.: 'Optimal design of C-type passive filters based on response surface methodology for typical industrial power systems', *Electr. Power Compon. Syst.*, 2013, **41**, (7), pp. 653–668
[30] Bradley N.: 'The response surface methodology'. MSc thesis, Indiana University South Bend, 2007

Appendix

The nameplate of the simulated IM and the results of its no-load and locked rotor tests are shown in Fig. 7.

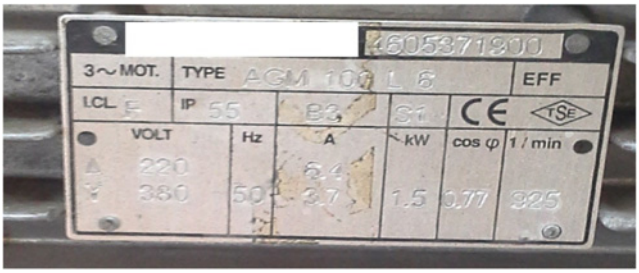

Test	Active power (W)	Voltage (V)	Current (A)
No-load test	319	380	2.35
Locked rotor test	415	97.68	3.71

Fig. 7 *Nameplate of the simulated IM and the results of its no-load and locked rotor tests*